



# Callose synthase and xyloglucan endotransglucosylase gene expression over time in *Citrus × clementina* and *Citrus × sinensis* infected with citrus tristeza virus

Melina da Silva · Sandra Germano ·  
Amílcar Duarte · Patrícia Pinto ·  
Natália Tomás Marques

Received: 12 October 2022 / Accepted: 13 March 2023  
© The Author(s) 2023

**Abstract** Citrus tristeza virus (CTV) is a virus that already caused great losses in citrus producing regions. The cell wall of plant cells plays an important role in the defence response to viruses. Following several studies indicating that cell wall enzyme transcripts of callose synthase 7 (*calS7*) and xyloglucan endotransglucosylase 9 (*xth9*) are modified during a viral infection, transcript expression of *calS7* isoform x5 (*calS7x5*) and *xth9* was evaluated over time in *Citrus × sinensis* ‘Valencia Late’ (VL) and *Citrus × clementina* ‘Fina’ (CL), infected with the severe CTV isolate T318A, by quantitative (q) PCR. qPCR analysis of healthy and CTV infected citrus was performed at 15 days, 10 months and at 31 months post-inoculation (dpi/mpi), respectively. The CTV titer, evaluated at the three time-points by qPCR, increased over time in bark tissues, with VL

plants exhibiting a titer about 5 times higher than CL 31 mpi. CTV infection did not cause significant changes in *calS7x5* gene expression over time in both citrus cultivars. However, CTV infection was associated with significant up-regulation of *xth9* in VL compared to controls 31 mpi. This study highlights that CTV infection can affect the expression of specific cell wall-associated genes over time and that this influence was distinct for VL and CL. This study provides further insight into the CTV-citrus host interaction, with the long-term response of VL to a severe CTV isolate involving a high expression of the *xth9* gene.

**Keywords** Callose synthase 7 · CTV · qPCR · Viral titer · Xyloglucan endotransglucosylase 9 · Gene expression

---

M. da Silva · N. T. Marques (✉)  
Centro de Eletrónica, Optoeletrónica e Telecomunicações,  
Universidade do Algarve, Edif. 8, Campus de Gambelas,  
8005-139 Faro, Portugal  
e-mail: nmarques@ualg.pt

M. da Silva  
e-mail: mcsilva@ualg.pt

S. Germano  
Universidade do Algarve, Campus de Gambelas,  
8005-139 Faro, Portugal  
e-mail: sandragermano@yahoo.com.br

A. Duarte  
Instituto Mediterrâneo para a Agricultura, Ambiente e  
Desenvolvimento, Universidade do Algarve, Campus de  
Gambelas, 8005-139 Faro, Portugal  
e-mail: aduarte@ualg.pt

P. Pinto  
Centro de Ciências do Mar, Universidade do Algarve,  
Campus de Gambelas, 8005-139 Faro, Portugal  
e-mail: ppinto@ualg.pt

## Abbreviations

act	$\beta$ -actin
ANOVA	Analysis of variance
CalS	Callose synthase
CalS7 x5	Callose synthase 7 isoform 5
CL	<i>Citrus</i> $\times$ <i>clementina</i> Hort. ex Tanaka 'Fina'
CTV	Citrus tristeza virus;
cox	Cytochrome c oxidase
DAMPs	Damage-associated molecular pattern
dpi	Days post-inoculation
dNTP's	Deoxyribonucleotides
dRNA	Defective RNA
GSL	Glucan synthase-like
mpi	Months post-inoculation
MYMIV	Mungbean yellow mosaic India virus
ORF	Open reading frame
PCR	Polymerase chain reaction
PD	Plasmodesmata
PVY	Potato virus Y
qPCR	Quantitative polymerase chain reaction, associated to real-time analysis
RT-PCR	Reverse transcription polymerase chain reaction
sgRNA	Sub-genomic RNA
SMV	Soybean mosaic virus
ssRNA(+)	Single-stranded genomic RNA of positive sense
totRNA	Total RNA
TuMV	Turnip mosaic virus
XET	Xyloglucan endotransglucosylase (activity)
XTH	Xyloglucan endotransglucosylase/hydrolase (protein)
XTH9	Xyloglucan endotransglucosylase 9
VL	<i>Citrus</i> $\times$ <i>sinensis</i> (L.) Osbeck 'Valencia Late'

## Introduction

Plants respond to a virus infection by inducing extensive defence mechanisms that determine the susceptibility or resistance to the pathogen (Kozieł et al., 2021). The cell wall plays an important role in this defence response, since it is a physical barrier to pathogens (Kozieł et al., 2021). The cell wall is composed of a network of cellulose and cross-linking glucans

embedded in a matrix of pectin polysaccharides (Houston et al., 2016). Cell walls of neighbouring cells are connected by plasmodesmata (PD), intercellular channels of 30–50 nm in diameter that establish a symplastic communication (Lee & Lu, 2011). The interaction of viruses with plant cells is accompanied by the deposition of callose, a  $\beta$ -1,3 glucan polymer in the PD, which reduces the orifice, thus blocking plasmodesmal trafficking and limit virus cell-to-cell movements (Lee & Lu, 2011). Callose may also be deposited on sieve elements, including the sieve plate, which limits the long-distance transport of viruses and contributes to increasing plant resistance (Zhang et al., 2022). The extent of changes that occur in the cell wall upon a viral infection are mirrored by the vast group of cell wall transcripts overexpressed, revealed by microarray gene expression and transcriptome analysis, that code for cellulose synthases, expansins, pectinesterases, xyloglucan endotrans-glucosylase/hydrolases, chitinases, callose synthase and glucanases (Chen et al., 2013; da Silva et al., 2023; Houston et al., 2016; Shimizu et al., 2007; Yadav & Chattopadhyay, 2014; Yang et al., 2007; Zheng et al., 2013).

Typical cell wall modifications that interfere with virus movement include cell wall thickening, alterations in its structure or permeability and changes in ion fluxes (Kozieł et al., 2021; Marwal & Gaur, 2020). In susceptible plants the virus is able to overcome the plant defence systems, such as the down-regulation of certain plant cell wall enzymes, facilitating systemic translocation of the virus (Chen et al., 2013; Shimizu et al., 2007; Yang et al., 2007; Zheng et al., 2013). Resistant plants prevent systemic movement of virus by mechanisms such as induced localized cell death and/or the accumulation of defensive wall-associated proteins such as pathogenesis-related proteins and deposition of cell-wall polysaccharides such as callose and xyloglucan (Otulak-Kozieł et al., 2018).

Callose is one of the most extensively studied polysaccharides associated with viral infections as its deposition in the PD, phloem sieve plates and other plant tissues controls cell-to-cell transport and slows virus invasion and movement (Iglesias & Meins, 2000; Li et al., 2012; Otulak-Kozieł et al., 2018; Zhang et al., 2022; Zheng et al., 2013). Viruses can also promote their intercellular movement in hosts by downregulating the synthesis of callose or promoting callose degradation at PD (Chowdhury et al., 2019).

Callose deposition is linked to pathogen-associated molecular patterns (PAMPs) recognition by the plant (Dalio et al., 2017). Most plant viruses move within sieve elements to achieve a systemic infection and massive callose deposition occurs in the sieve tube plates within minutes of infection, to control or stop pathogen transport (Kloth & Kormelink, 2020; Zhang et al., 2022). The linear polymer of  $\beta$ -1,3-glucans is synthesized by a complex of enzymes where callose synthase (CalS) is the catalytic subunit (Nedukha, 2015). In *Arabidopsis thaliana* 12 distinct isoforms of *calS* have been identified and their expression is dependent on the tissue type, developmental stage and the presence of biotic and abiotic stresses (Barratt et al., 2011; Nedukha, 2015; Piršelová & Matušíková, 2013; Töller et al., 2008). Among the three enzymatic isoforms with a role in callose deposition, callose synthase 7 [CalS7 or glucan synthase-like 7 (GSL7)] is most active in phloem cells and is responsible for callose synthesis in PD and in sieve plates (De Storme & Geelen, 2014). Callose deposition occurs during phloem formation and as a result of wounding, in different plant organs, including the stem tissue (Barratt et al., 2011; De Storme & Geelen, 2014; Nedukha, 2015; Piršelová & Matušíková, 2013; Töller et al., 2008; Xie et al., 2011). The function of CalS7 was revealed by mutants lacking the enzyme, which showed reduced accumulation of callose in the phloem sieve plates, on the radial walls of the sieve elements and in companion cells (De Storme & Geelen, 2014). *CalS7* transcript expression was up-regulated with viral infection in several herbaceous (Babu et al., 2008; Chen et al., 2013; Otulak-Kozielec et al., 2018; Shimizu et al., 2007; Wu et al., 2013) and woody plants (Allie et al., 2014; Madroñero et al., 2018).

Xyloglucan is the predominant hemicellulose in the cell walls and contributes to wall assembly and growth regulation, making the cell wall more rigid when it is cross-linked to cellulose fibres (Fry et al., 1992; Hayashi & Kaida, 2011). This polysaccharide, formed by a 1,4- $\beta$ -glucan backbone with 1,6- $\alpha$ -xylosyl residues, is present in the middle lamella, primary walls, and gelatinous wall layer of cell walls (Hayashi & Kaida, 2011). Changes in the metabolism of xyloglucan occurs in the presence of viruses (Otulak-Kozielec et al., 2018; Yadav & Chattopadhyay, 2014; Zheng et al., 2013). Xyloglucan endotransglucosylase/hydrolases (XTHs) are

enzymes with hydrolytic activities (XEH) and cross-linking activities (XET) responsible for splitting and assembly of the xyloglucan crosslinks in the cell wall (Kaur, 2019; Sharples et al., 2017).

Plants belonging to the genus *Citrus* (family Rutaceae), cultivated in tropical and subtropical areas, are the most commercially important woody fruit crops in the world (Liu et al., 2012) and are part of the Mediterranean diet (Duarte et al., 2016). The productivity and longevity of citrus species has been severely affected in citrus producing regions by a commonly distributed virus, citrus tristeza virus (family *Closteroviridae*, genus *Closterovirus*), which has a single-stranded positive-sense RNA genome (approx. 19.3 Kb) (Karasev et al., 1995; Z. N. Yang et al., 1999). Citrus tristeza virus (CTV) isolates may cause one of four distinct syndromes in *Citrus* spp.: decline or tristeza disease (which may induce plant death), stem pitting (abnormal phloem development), seedling yellows (leaf chlorosis and stunting) or an absence of symptoms (Dawson et al., 2015). CTV infection is mainly restricted to phloem cells, although the virus was also found in tracheid cells. CTV replicates in companion cells or phloem parenchyma cells and systemic infection is by long-distance movement in sieve elements (Folimonova, 2020). However, there is a poor understanding of the changes in the composition of the cell wall of phloem cells in face of an infection triggered by CTV. Cell-to-cell and long-distance movement of CTV in phloem cells has been found to depend on the citrus host genotype and the host-virus interaction, with several viral proteins participating, including p33, p13 and p18 (Dawson et al., 2015; Folimonova et al., 2008; Folimonova, 2020; Tatineni et al., 2011). Exposure of the highly susceptible *C. macrophylla* to CTV clone T36-GFP resulted in small clusters of infected companion cells, while the sour orange (*C. aurantium*), which has low susceptibility to CTV, displayed limited cell-to-cell viral movement (Folimonova et al., 2008). Furthermore, sour orange seems to have a transient viral resistance to CTV which lasts for about two years, after which severe CTV isolates such as T36 and mild isolates show a viral titer similar to that of Mexican lime (Albiach-Martí, 2012). Comparative transcriptome profiling analysis revealed that *calSs* and *xthS* transcripts, as well as transcripts encoding cellulose synthase and expansins, were induced when *C. × sinensis* was infected with pathogens including CTV,

although the response differed with the isolate (mild with CTV-B2 or severe with CTV-B6) (Cheng et al., 2016; Fu et al., 2016, 2017; Granato et al., 2019).

*Citrus × clementina* (CL) ‘Fina’ and *Citrus × sinensis* ‘Valencia Late’ (VL) are widely planted citrus cultivars. The present study evaluated the expression of callose synthase 7 isoform 5 (*calS7x5*) and xyloglucan endotransglucosylase 9 (*xth9*) genes over time in the two citrus cultivars, infected with the severe stem pitting CTV isolate T318A. *CalS7x5* and *xth9* gene expression were evaluated by quantitative (q) PCR in CL and VL bark tissue of healthy and CTV infected citrus, after 15 days, 10 months and 31 months post-inoculation (dpi/mpi, respectively), to guarantee that both short-term and long-term responses were covered. The CTV titer in control and inoculated CL and VL plants were also evaluated and revealed that VL reached a viral titer 4.9 times higher than CL at 31 mpi. The results revealed that the two citrus cultivars had a different response to CTV infection and that *xth9* gene expression may play a role in CTV infection.

## Material and methods

### Plant material and virus isolate

*Citrus × clementina* hort. ex Tanaka ‘Fina’ (CL) and *Citrus × sinensis* (L.) Osbeck ‘Valencia Late’ (VL), grafted onto the rootstock ‘Carrizo’ citrange (*Citrus × sinensis* Osb. × *Citrus trifoliata* L.), were purchased from a certified CTV-free nursery and then maintained into a greenhouse at the University of Algarve. These two-year-old plants were potted in a 50:50 mix of pine bark and coconut fiber, fertilized one time a week and kept in an insect-proof greenhouse. Plants were maintained under normal ambient conditions (temperature, relative humidity and illumination) for the Algarve region, Portugal, from April 2014 to March 2017. Two groups of four plants were used in this study for each citrus cultivar, CL and VL. One group of four plants of each cultivar was infected with the severe stem pitting CTV isolate T318A from VT genotype (Harper, 2013), kindly provided by Dr. Leandro Peña (Institute for Plant Molecular and Cell Biology – Polytechnic University of Valencia) and the other groups were the control and were not inoculated with CTV.

CL and VL were infected with CTV as described in Afonso et al. (2017). Samples from each group were collected at three different post-CTV inoculation times: 15 days post-inoculation (dpi), 10 months post-inoculation (mpi), and 31 mpi. Sampling of young twigs at approximately the same stage of development from each plant occurred in November (15 dpi), September (10 mpi) and June (31 dpi).

### Molecular methods

#### Total RNA extraction

Total RNA (totRNA) was extracted from 100 mg of slices from young bark tissue (herbaceous material) of control and infected plants using TRI Reagent (Sigma-Aldrich, USA) according to the manufacturer’s instructions, and stored at -80 °C until use. totRNA (5 µg) extracted from each sample was treated with a TURBO DNA-free™ Kit (Ambion, Germany) according to the manufacturer’s instructions, to eliminate DNA contamination. The integrity of the RNA samples was assessed by gel electrophoresis and the concentration of RNA was determined using a NanoPhotometer® UV–Vis Spectrophotometer (IMPLEN, Germany).

#### Detection of CTV by RT-PCR

Confirmation of the CTV infection status of the citrus plants, CL and VL, was evaluated by amplification of the coat protein (p25) gene of CTV using reverse transcription polymerase chain reaction (RT-PCR). The RT-PCR reaction was performed using degenerate primer pairs to amplify the complete sequence (672 bp) of the p25 gene (Table 1). The RT-PCR reaction mixture and programme was performed as described before (Afonso et al., 2017). Two µL (50 ng/µL) of totRNA were used from each sample analysed. The RT-PCR amplicon was purified using a MEGAquick-spin™ Plus Total Fragment DNA Purification Kit (GE Healthcare, UK), following the manufacturer’s instructions. The amplicon was cloned into a pGEM-T Easy vector (Promega, USA), sequenced and aligned with the reference sequence of isolate T318A retrieved from GenBank (GenBank accession DQ151548) and using ClustalX.

**Table 1** Primer sequences used in RT-PCR, PCR and qPCR amplifications and their respective efficiency and R<sup>2</sup> value of the standard curve (for qPCR)

Amplified sequence	Primer 5'-3'	Amplicon size (bp)	Efficiency (%)	R <sup>2</sup>	Reference
CTV Detection					
<i>p25</i> (CTV)	Fw ATGGACGACGARACAAAG Rv TCAACGTGTGTTAATTTCC	672	–	–	This work
Primers for cloning into pGEM T-Easy					
<i>calS7x5</i>	Fw TGTTGCGTGGACTTCTGATG Rv TCTTCCAACATACAGTTTCGGC	397	–	–	This work
<i>xth9</i>	Fw TCTGCTGGAAGTCTACTG Rv GCCCAGTCATCAGCATTCCA	341	–	–	This work
Real-time qPCR primers 5'-3'					
<i>act</i>	Fw CAGTGTGGATTGGAGGATCA Rv TCGCCCTTGAGATCCACAT	74	97.3	0.998	(Agüero et al., 2014)
<i>cox</i>	Fw GTATGCCACGTCGCATTCCAGA Rv GCCAAAAGTCTAAGGGCATTCC	68	98.5	0.999	(Li et al., 2006)
<i>calS7x5</i>	Fw ATAGGGTTCTCCAGGTTCTGA Rv GCTTCACCCAGATAAGAAGA	81	104.2	0.993	This work
<i>xth9</i>	Fw GTGAATGGTGTGGGCAACAGAGAG Rv TCCTTTGTGCTCCAAGTTAGTGTGC	156	92.8	1	This work
<i>ORF1a-2b</i> (CTV)	Fw CGCGTGGGTTATTTTCGTAC Rv CGAAGGCAAACATCTCGACTC	148	99.4	0.999	(Ruiz-Ruiz et al., 2007)

Fw forward primer; Rv reverse primer. R = A/G; Y = C/T

### Synthesis of cDNA and amplification of CTV *ORF1a-2b* and citrus genes *calS7x5* and *xth9*

To perform reverse transcription for transcript expression analysis, totRNAs from all samples of the experiment (including all time-points and the two cultivars) were denatured at 65 °C for 5 min and ice cooled for another 5 min. Reverse transcription reactions were performed using the same reactional mix for all samples, in a final reaction volume of 20 µL using 500 ng of denatured totRNA, 200 ng of random hexamers (Jena Bioscience, Germany), 500 µmol of dNTPs (Invitrogen, USA), 8 U of RiboLock RNase Inhibitor (Thermo Scientific, USA) and 100 U of RevertAid Reverse Transcriptase (Thermo Scientific, USA). Reverse transcription reactions occurred at 42 °C for 1:30 h, followed by enzyme inactivation at 70 °C for 10 min.

Sequences of CTV *ORF1a-2b* and citrus genes *calS7x5* and *xth9* were amplified by PCR and cloned into the pGEM T-Easy vector and used for standard curves in real-time PCR analysis. Primers designed for CTV *ORF1a-2b* (Table 1) did not amplify sgRNAs (3' coterminal sgRNAs) and dRNAs (Ruiz-Ruiz

et al., 2007). PCR reactions had a final volume of 15 µl and contained 2 µL of cDNA (0.5–1 µg), 200 nmol of each primer (Table 1), 200 µM of each dNTP (Invitrogen) and 0.375 U of BioTaq (BioLine, UK). The amplification reactions were performed in a thermal cycler T100™ (BioRad, USA) using the following cycle: 95 °C for 2 min, followed by 35 cycles at 95 °C for 30 s, 60 °C for 35 s, and 72 °C for 40 s, with a final extension time of 7 min at 72 °C. A negative control reaction without cDNA was included. A PCR product with the predicted amplicon size was gel purified and cloned into the pGEM T-Easy vector as described above, sequenced and the identity of the amplicon confirmed by searching against the NCBI database (<http://blast.ncbi.nlm.nih.gov/Blast.cgi>) using the Blastn algorithm.

A partial sequence of callose synthase 7-like, transcript variantx5, of 397 bp, was amplified from CL and VL cDNA by PCR using the primers for *calS7x5* (Table 1), designed to amplify a nucleotide region with no homology to other *calS7* isoforms (GenBank accession: XR\_008054095). Amplified CL and VL callose synthase sequences were aligned using ClustalW software (<http://www.genome.jp/tools/clust>

alw/) and used to design primers for quantitative real-time PCR (qPCR). Isolation of xyloglucan endotransglucosylase/hydrolase 9 (XTH9) (GenBank accession: XM\_006447384) used specific primers and the same strategy as outlined above (Table 1). PCR reactions had a final volume of 15 µl and the same reaction conditions and cycle conditions described above, except for the annealing temperature that was 58 °C for both *calS7x5* and *xth9*. A negative control reaction without cDNA was included. PCR products with the predicted amplicon size were gel purified and cloned into the pGEM T-Easy vector as described above, sequenced and their identity confirmed using Blastn against the NCBI database (<http://blast.ncbi.nlm.nih.gov/Blast.cgi>).

#### Real-time quantitative PCR (qPCR)

qPCR assays were designed to quantify the expression of *calS7x5* and *xth9* in healthy or infected CL and VL plants, using the specific primers in Table 1. qPCR analysis was also performed for ORF1a-2b from CTV isolate T318A. Samples from 15 dpi, 10 mpi and 31 mpi ( $n=4/\text{time-point}$ ) and control CL and VL plants were analysed by qPCR.

All qPCR reactions were performed in duplicate using a StepOnePlus™ Real-Time PCR thermocycler (Applied Biosystems, USA) using EvaGreen chemistry (BioRad, USA). The qPCR reaction mix contained 5 µL of 2×Sso Fast EvaGreen Supermix (BioRad, USA), 2.4 µL of RNase free water, 2 µL of synthesized cDNA (diluted 1:5) and 300 nM of each primer pair (Table 1) in a final volume of 10 µL. The cycling conditions were 30 s at 95 °C, 40 cycles of 5 s at 95 °C and 10 s at the optimal annealing temperature for the primers (58 °C for *calS7x5*, *xth9* and *cox* and 60 °C for CTV and *act*), followed by a final melting curve between 65 °C and 95 °C. A standard curve relating amplification cycle with initial template quantity, determined by NanoPhotometer® UV-Vis Spectrophotometer (IMPLEN, Germany), was prepared using tenfold serial dilutions of each amplicon. Copy number was determined using the following equation:

$$\text{number of copies} = \frac{X \times NA}{Y \times 1 \times 10^9 \times 650}$$

where X is the initial template concentration (ng of the amplicon fragment), NA is Avogadro's number, Y is the template length (bp of each amplicon), and

650 (Da) is the average weight of a base pair (Afonso et al., 2017). Before calculating copy number for each duplicate reaction, it was verified that the average standard deviation between replicate Cts was below 0.5 and their maximum levels generally below 1. Samples where gene levels were very low (Ct above 35, such as the case of the CTV levels in control plants) had higher standard deviation levels and were considered as zero, after this revision.

The reference genes *act* and *cox* were used to normalize the expression of the target genes (Table 1), after confirming their expression levels was stable across all samples, using the *BestKeeper* software (Pfaffl et al., 2004) at the web-based RefFinder resource at <http://blooge.cn/RefFinder/> (Xie et al., 2012). The *BestKeeper* gene stability values for *act*, *cox* and their geometric mean were 0.87, 0.99 and 0.92, respectively. Despite the slightly higher stability of the *cox* gene alone, it was decided to normalize all data by the geometric mean of the two validated stable reference genes, since it is recommended for an accurate qPCR to use more than one reference gene (Vandesompele et al., 2002). Relative gene expression of *calS7x5* and *xth9* levels in each plant and condition was calculated by dividing gene copy number by the geometric mean of the copy number of the reference genes, *cox* and *act*, in each sample (Pfaffl et al., 2004). All qPCR efficiencies were >90% and the regression coefficients ( $R^2$ ) of standard curves was >0.99 (Table 1). The melting curve of each amplicon had a single peak and confirmed the absence of significant secondary primer structures or nonspecific amplification products. No PCR products were detected when cDNA synthesis was carried out without reverse transcriptase (-RT control) or when the cDNA template was omitted.

#### Statistical analysis

Results are presented as the mean ± SEM (CL-15dpi-control  $n=3$ ; CL-15dpi-infected  $n=4$ ; CL-10mpi-control  $n=3$ ; CL-10mpi-infected  $n=4$ ; CL-31mpi-control  $n=3$ ; CL-31mpi-infected  $n=4$ ; VL-15dpi-control  $n=3$ ; VL-15dpi-infected  $n=4$ ; VL-10mpi-control  $n=3$ ; VL-10mpi-infected  $n=3$ ; VL-31mpi-control  $n=3$  and VL-31mpi-infected  $n=4$ ), using SigmaPlot v12 (SPSS Inc.). Statistical analysis of the expression of each gene within

one cultivar was assessed using two-way analysis of variance (ANOVA) with time post-inoculation and infection status as factors and the software SigmaPlot version 14.0. Significant statistical differences were accepted when the  $p$ -value was  $<0.05$  and were evaluated by Multiple Comparisons (Tukey Test) versus the control condition, which was defined as 15 dpi for the factor “time post-inoculation” and as the control (non-infected) group for the factor “infection status” for both cultivars.

## Results and discussion

CTV titer in ‘Valencia Late’ sweet orange and ‘Fina’ clementine over time

The CTV titer in citrus cultivars CL and VL increased over time, reaching a significantly higher titer at 31 mpi, compared with the other two time-points and non-infected individuals (Fig. 1). Fold change analysis revealed VL generally had a higher CTV titer than CL (Fig. 1 and Table 2). The relative quantification of CTV in VL and CL was evaluated at each sample time-point (Table 2). Values of CTV titer at 15 dpi were low in both CL and VL but at this early stage of infection VL plants already exhibited, in terms of relative quantification,

**Table 2** Comparison between relative CTV quantification in CL and VL plants at 15 dpi, 10 mpi and 31 mpi

Time post-inoculation	Cultivars		Ratios	
	CL	VL	CL/VL	VL/CL
15dpi	$1.80 \times 10^{-2}$	$6.04 \times 10^{-1}$	$3.14 \times 10^{-1}$	$3.19 \times 10^1$
10mpi	$1.09 \times 10^5$	$4.19 \times 10^5$	$2.60 \times 10^0$	$3.84 \times 10^{-1}$
31mpi	$2.01 \times 10^5$	$9.98 \times 10^5$	$2.01 \times 10^{-1}$	$4.97 \times 10^0$

a CTV titer 30 times higher than CL (Table 2). At 10 mpi, the relative titer of CTV was slightly lower in VL, but after 31 mpi VL plants had 5 times higher CTV than CL (Table 2), levels that for both cultivars represented a significantly higher titer at 31 mpi compared to the previous time-points (Fig. 1). As previously demonstrated, CTV-infected citrus hosts usually show high viral titers during spring and autumn (Cambra et al., 2002), which may explain the high viral titers in CL and VL samples collected in June, at 31 mpi. The nucleotide sequence of the CTV p25 gene of isolate T318A was confirmed by sequencing. The specificity of the primers avoided the amplification of abundant sgRNAs that form during CTV replication. These sgRNAs consist of the (-) ssRNAs complementary to the gRNA, the positive and negative strands of the ten 3' co-terminal sgRNAs and

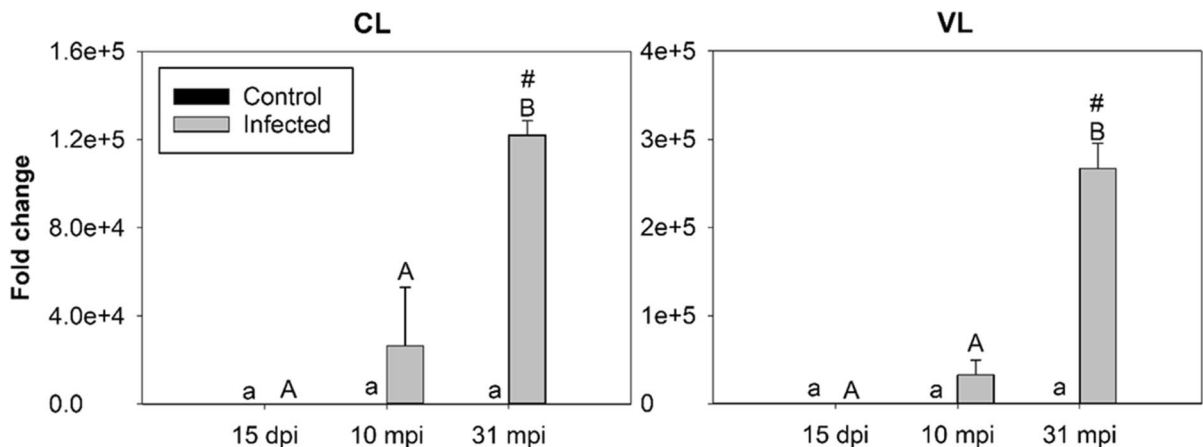


**Fig. 1** Relative quantification by qPCR of CTV in young bark tissue from CL and VL infected with the severe CTV isolate T318A at 15 dpi, 10 mpi and 31 mpi, and the respective controls. Relative quantification of CTV in each group of plants, was obtained using CTV copy number normalized by the copy number of the internal controls *act* and *cox*. The mean and standard deviation were obtained using four biological replicates and two independent assays. The same lower-case letters

indicate relative CTV titer that are not significantly different ( $p < 0.05$ ) in control plants compared along the different time-points. Different upper-case letters indicate relative CTV titer that is significantly different ( $p < 0.05$ ) between CTV infected plants, at the indicated time. # represents a statistically significant difference ( $p < 0.05$ ) in CTV titer between CTV infected plants and their respective control, at the indicated times post-inoculation

the two abundant positive-stranded 5′ co-terminal RNA species of ~800 nt each one (Ruiz-Ruiz et al., 2007).

Sampled plant material was from young branches with tender bark, known to contain the highest virus titer (Korkmaz et al., 2008; Zhou et al., 2017). The time of inoculation with CTV was 2.7 years prior to the last sampling, so the virus was expected to be evenly distributed in all parts of the host plant. The CTV viral titer also depends on the activity of the viral suppressor genes p23, p20 and p25 that interact with the antiviral RNA silencing mechanisms as well as on the products of the viral genes p33, p18 and p13 whose function are not completely understood (Dawson et al., 2013). Mechanisms such as salicylic acid and enzymatic and non-enzymatic antioxidant activities also interfere with viral titer (Gómez-Muñoz et al., 2017; Munir et al., 2019). The difference in CTV viral titer between VL and CL are also related to the citrus cultivar. Different citrus species support different CTV titers as revealed for the susceptible hosts *C. macrophylla* and *C. × sinensis* ‘Madam Vinous’ and the low susceptible host sour orange, which was associated with the ability of the virus to infect phloem companion cells and to move in the sieve elements (Dawson et al., 2013; Folimonova et al., 2008). Viral accumulation inside the host depends also on the CTV isolate, and particularly T318A has been shown to increase its viral load in sour orange, sweet orange, *C. macrophylla* and *C. aurantifolia* (Mexican lime) in the first two years, stabilizing at 2.5 years (Comellas, 2009). Despite the possible initial dissimilar CTV accumulation in different citrus tissues (Dawson et al., 2015), a high and stabilized CTV titer was determined in sour orange and sweet orange genotypes at 36 mpi, infected with mild or severe stem pitting isolates as T318A and T36 (Comellas, 2009). The viral titer values for CL and VL at 31 mpi, point to the conclusion that VL is more susceptible to CTV than CL.

#### Expression of *calS7x5* and *xth9* genes in citrus cultivars over time and CTV infection

Both CL and VL showed no change in their phenotype over the 31-month study period. In the present study it was found that *calS7x5* gene expression in CL cultivar was significantly different between infected and non-infected plants only at 15 dpi, with infected plants showing a lower expression, denoted by a # (Fig. 2). Both CL and VL plants displayed an increased expression of *calS7x5* at 10 mpi, compared to the previous sampling

time, equally for infected and healthy plants. The expression of *calS7x5* at 31 mpi was identical to infected and control plants for both citrus cultivars (Fig. 2). These results do not agree to what was previously described in *C. × sinensis* infected with the CTV severe isolate B6, where it was found the up-regulation of transcripts encoding an enzyme that indirectly promoted callose deposition (Fu et al., 2016). The distinct response of the VL cultivar of *C. × sinensis* could be related to the type of tissue studied, in this case the stem and not the leaf (analysed by Fu et al., 2016). On the other hand, distinct CTV isolates may cause different symptoms in the same citrus host (Dawson et al., 2015), and B6 and T318A are distinct, although belonging to the same VT genotype (Harper, 2013). As reported by Fu et al. (2017), the mild isolate B2 and the severe isolate B6 induce distinct transcripts in *C. × sinensis* related to the synthesis of cell wall enzymes as cellulose synthase. The results of this study indicate that the infection of VL and CL with a severe CTV isolate do not interfere in *calS7x5* gene expression, at least at the analysed time-points.

The outcome of a viral infection caused by both the mild B2 and the severe B6 CTV isolates in *C. × sinensis* induced transcripts encoding xyloglucan endotransglycosylase/hydrolase (XTH) (Fu et al., 2016). However, it seems an increase in *xth* gene expression is not a common feature to all CTV infected citrus species as *C. macrophylla* infected with T318A showed a lower expression of *xth9* transcripts in the bark stem tissues at 14 mpi (da Silva et al., 2023). In the present work, *xth9* gene expression was found highly expressed in infected plants of both cultivars CL and VL at 15 dpi (Fig. 2). At 31 mpi, both cultivars exhibited statistically significant differences in *xth9* gene expression compared to the respective control plants, with a down-regulation in CL and a noticeable up-regulation in VL (Fig. 2). It should be noted that control VL plants showed an almost constant *xth9* gene expression at the three time-points examined (Fig. 2). The high *xth9* gene expression detected in VL could be related to the need for xyloglucans availability, possibly involved in a response to CTV infection. The hemicellulose xyloglucan was reported to be part of the endogenous elicitors involved in a signalling cascade of defence responses to pathogens in *Vitis vinifera* and *Arabidopsis*, which includes activation of MAPK pathways and phenylalanine ammonia-lyase (PAL) that catalyses the first step of the phenylpropanoid pathway (Claverie et al., 2018). The attained results suggest that the

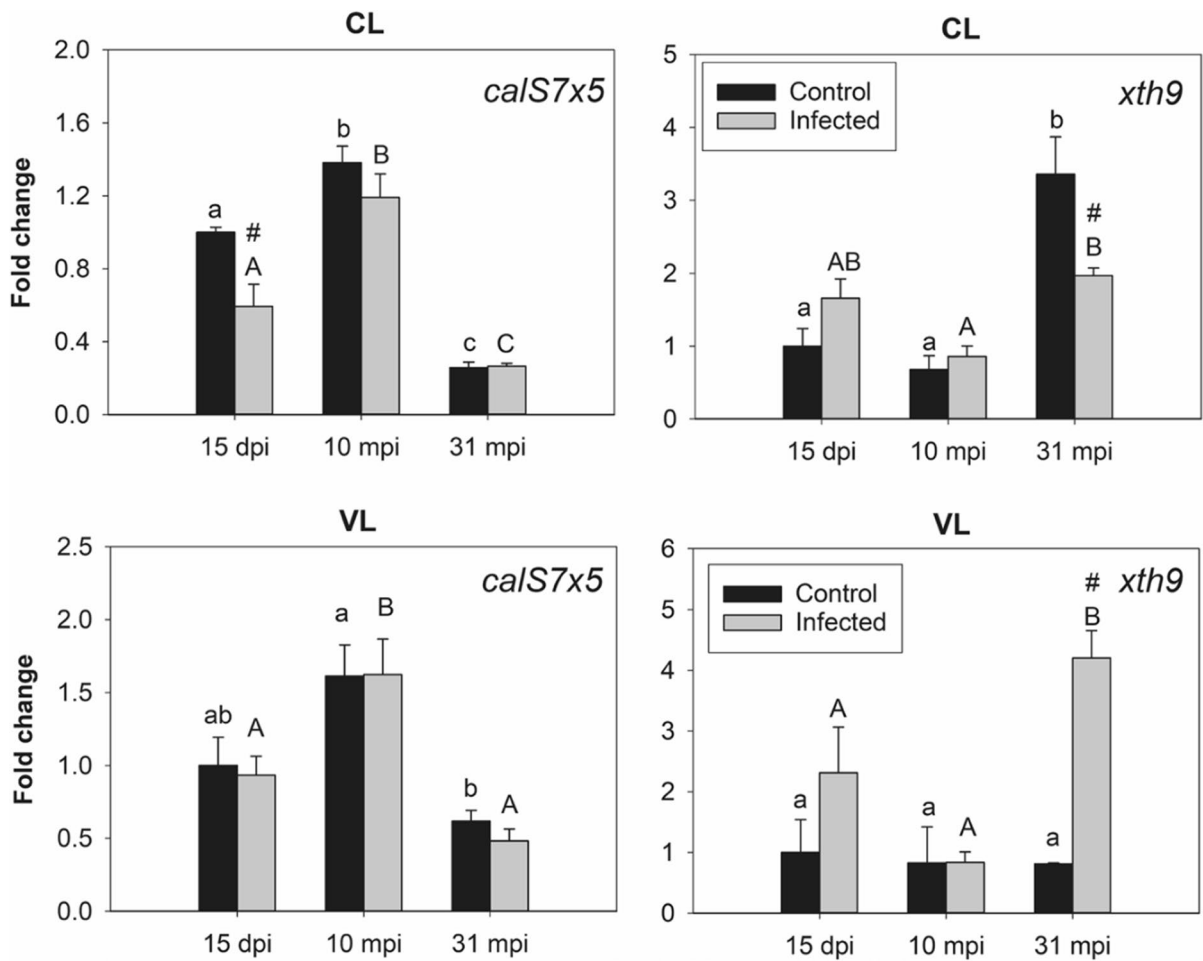


**Fig. 2** Relative quantification of *calS7x5* and *xth9* in young bark tissue from 'Fina' clementine (CL) and 'Valencia Late' (VL) healthy and infected plants with the severe CTV isolate T318A, at 15 dpi, 10 mpi and 31 mpi, estimated by qPCR. Represented values are the relative quantification of CTV in each plant group, in copy number normalized by the copy number of the internal controls *act* and *cox*. Means and standard deviations were obtained from four biological replicates and two independent assays. Different lower-case letters

indicate a statistically significant difference for gene expression ( $p < 0.05$ ) of each gene in control plants over time. The same type of notation but using upper-case letters was used to express significantly different expression levels when comparing infected plants along different time-points (temporal changes in the infected group). # represents a statistically significant difference ( $p < 0.05$ ) of expression between control and CTV infected plants at the indicated times post-inoculation

increase in *xth9* gene expression in VL is related to a citrus defence response. In soybean plants affected by the soybean mosaic virus, a fluctuation of callose synthase transcripts over time was described, which were repressed at 7 dpi and induced at 14 dpi, inferred to be a delayed resistance response from the infected plant (Babu et al., 2008). Callose deposition related to the occlusion of sieve elements is a labile process that changes in a question of minutes or hours (Kloth

& Kormelink, 2020; Walker, 2022). The evaluation of *calS7x5* and *xth9* gene expression took place at 15 dpi followed by well separated times, so it may not have captured changes that may have occurred shortly after the onset of infection. Factors that may have influenced *calS7x5* and *xth9* gene expression variability over time was exposure to different temperature and humidity conditions, which changed depending on the season the plants were sampled. As an example, a callose

synthase gene expression changed with the flowering stage of *Carica papaya* (Madroñero et al., 2018).

The present results confirm that the two citrus cultivars respond differently to CTV T318A infection, resulting in a distinct viral titer at 31 mpi for VL, 4.9 higher than for CL (Table 2). Based on previous reports regarding infection of *C. macrophylla* and sour orange with a T36 cDNA clone, where a high CTV load evidenced a susceptible host (Dawson et al., 2013; Folimonova et al., 2008), it is suggested that the enzyme encoded by gene *xth9* may contribute to a successful CTV infection in VL. A lower *xth* gene expression was described in *Arabidopsis* in response to an infection with turnip mosaic virus (TuMV) (Yang et al., 2007) and in soybean in response to mungbean yellow mosaic India virus (MYMIV) (Yadav & Chattopadhyay, 2014). Contrarily, the potato virus Y (PVY) infection redirected the deposition of XTH5 compared to control plants (Otulak-Kozieł et al., 2018). In the case of *C. × sinensis*, it was previously reported that an infection with CTV increased cell wall metabolism-related genes (Cheng et al., 2016), where *xth6*, *xth28* and *xth30* were found up-regulated in response to both mild and severe isolates (Fu et al., 2017).

## Conclusions

CL and VL plants infected with the severe isolate T318A showed an increase in viral titer over time and after more than 2.5 years post-inoculation with CTV. CTV replication was distinct among the two citrus cultivars, with VL having a viral titer approximately 5 times higher than that of CL at 31 mpi, which suggests that VL is more susceptible to CTV than CL. A temporal variation in *calSx5* gene expression over time was depicted in both controls and infected plants of CL and VL, which occurred in a similarly way, so these changes seemed to be independent of CTV infection. *calS7x5* gene expression was underexpressed at 31 mpi, when both citrus cultivars had a high viral titer. Our experiment revealed a significant impact of CTV infection on *xth9* gene expression for both citrus cultivars after 31 mpi. A significant increase of *xth9* gene expression was detected in VL infected plants compared to its controls, while in infected CL *xth9* gene expression was significantly decreased. This

study points to a very distinct response of VL and CL to CTV infection, which seems to involve *xth9* gene expression. Our hypothesis is that the increased *xth9* gene expression in VL over time is related to a citrus defence response. Many aspects related to the complex CTV-host interaction still need to be unraveled. The specificity is such that different CTV isolates interact differently with the same citrus host, as well as the same isolate can induce different symptoms in different citrus hosts. It will be interesting in the future to investigate if and how *xth9* gene expression could impact on the susceptibility of VL to CTV.

**Acknowledgements** Authors would like to acknowledge Diamantino Trindade and Fernando André from nursery Mil Plantas for providing the citrus plants.

**Author's contributions** Natália Marques and Patrícia Pinto designed the experiment. Amílcar Duarte graft-inoculated citrus plants. Sandra Germano and Melina Silva performed the RNA extraction and gene expression analysis. Melina Silva, Patrícia Pinto and Natália Marques analysed, interpreted the data and drafted the manuscript. Melina Silva, Patrícia Pinto, Amílcar Duarte and Natália Marques revised the manuscript. All authors reviewed and edited the manuscript. Natália Marques secured the financing.

**Funding** Open access funding provided by FCTIFCCN (b-on). Melina Silva and Sandra Germano were funded by UIDB/00631/2020 CEOT BASE, Universidade do Algarve, Portugal. Patrícia Pinto was funded by “Fundação para a Ciência e a Tecnologia” (FCT) under the “Norma Transitória” -DL57/2016/CP1361/project CT0015. This study received Portuguese national funds from FCT through project PTDC/BAA-AGR/30957/2017, and from the Investment and Structural European Funds (FEEI) by Portugal 2020 – Algarve’s Regional Operational Programme (CRESC 2020) through project ALG-01-0145-FEDER-30957. This study was partially funded by FCT/UID/Multi/04326/2020/CCMAR.

**Data availability statement** All data and materials from this research generated or analyzed during this study are available in this article or from the corresponding author upon reasonable request.

## Declarations

**Competing interests** The authors declare no competing interests.

**Ethics approval** Not applicable.

**Consent to participate** Not applicable.

**Consent for publication** Authors grant all consents to publish the manuscript.

**Conflicts of interest** The authors declare no conflicts of interest.

**Open Access** This article is licensed under a Creative Commons Attribution 4.0 International License, which permits use, sharing, adaptation, distribution and reproduction in any medium or format, as long as you give appropriate credit to the original author(s) and the source, provide a link to the Creative Commons licence, and indicate if changes were made. The images or other third party material in this article are included in the article's Creative Commons licence, unless indicated otherwise in a credit line to the material. If material is not included in the article's Creative Commons licence and your intended use is not permitted by statutory regulation or exceeds the permitted use, you will need to obtain permission directly from the copyright holder. To view a copy of this licence, visit <http://creativecommons.org/licenses/by/4.0/>.

## References

- Afonso, A. M., Guerra, R., Cavaco, A. M., Pinto, P., Andrade, A., Duarte, A., & Marques, N. T. (2017). Identification of asymptomatic plants infected with *Citrus tristeza virus* from a time series of leaf spectral characteristics. *Computers and Electronics in Agriculture*, *141*, 340–350. <https://doi.org/10.1016/j.compag.2017.08.001>
- Agüero, J., del Carmen Vives, M., Velázquez, K., Pina, J. A., Navarro, L., Moreno, P., & Guerri, J. (2014). Effectiveness of gene silencing induced by viral vectors based on *Citrus leaf blotch virus* is different in *Nicotiana benthamiana* and citrus plants. *Virology*, *460–461*, 154–164. <https://doi.org/10.1016/j.virol.2014.04.017>
- Albiach-Martí, M. R. (2012). Molecular virology and pathogenicity of *Citrus tristeza virus*. In M. L. Garcia & V. Romanowski (Eds.), *Viral genomes - molecular structure, diversity, gene expression mechanisms and host-virus interactions*. IntechOpen. <https://doi.org/10.5772/27052>
- Allie, F., Pierce, E. J., Okoniewski, M. J., & Rey, C. (2014). Transcriptional analysis of *South African cassava mosaic virus*-infected susceptible and tolerant landraces of cassava highlights differences in resistance, basal defense and cell wall associated genes during infection. *BMC Genomics*, *15*(1), 1006. <https://doi.org/10.1186/1471-2164-15-1006>
- Babu, M., Gagarinova, A. G., Brandle, J. E., & Wang, A. (2008). Association of the transcriptional response of soybean plants with soybean mosaic virus systemic infection. *The Journal of General Virology*, *89*(Pt 4), 1069–1080. <https://doi.org/10.1099/vir.0.83531-0>
- Barratt, D. H. P., Kölling, K., Graf, A., Pike, M., Calder, G., Findlay, K., Zeeman, S. C., & Smith, A. M. (2011). Callose synthase *GSL7* is necessary for normal phloem transport and inflorescence growth in *Arabidopsis*. *Plant Physiology*, *155*(1), 328–341. <https://doi.org/10.1104/pp.110.166330>
- Cambra, M., Gorris, M. T., Olmos, A., Martínez, M. C., Román, M. P., Bertolini, E., López, A., & Carbonell, E. A. (2002). European diagnostic protocols (DIAGPRO) for *Citrus tristeza virus* in adult trees. *International Organization of Citrus Virologists Conference Proceedings*, *15*(15), 69–73. <https://doi.org/10.5070/c54ph9b2xr>
- Chen, T., Lv, Y., Zhao, T., Li, N., Yang, Y., Yu, W., He, X., Liu, T., & Zhang, B. (2013). Comparative transcriptome profiling of a resistant vs. susceptible tomato (*Solanum lycopersicum*) cultivar in response to infection by *Tomato yellow leaf curl virus*. *PLOS ONE*, *8*(11), e80816. <https://doi.org/10.1371/journal.pone.0080816>
- Cheng, C., Zhang, Y., Zhong, Y., Yang, J., & Yan, S. (2016). Gene expression changes in leaves of *Citrus sinensis* (L.) Osbeck infected by *Citrus tristeza virus*. *The Journal of Horticultural Science and Biotechnology*, *91*(5), 466–475. <https://doi.org/10.1080/14620316.2016.1173523>
- Chowdhury, R. N., Lasky, D., Karki, H., Zhang, Z., Goyer, A., Halterman, D., & Rakotondrafara, A. M. (2019). HCPPro suppression of callose deposition contributes to strain-specific resistance against *Potato virus Y*. *Phytopathology*, *110*(1), 164–173. <https://doi.org/10.1094/PHYTO-07-19-0229-FI>
- Claverie, J., Balacey, S., Lemaître-Guillier, C., Brulé, D., Chiltz, A., Granet, L., Noirot, E., Daire, X., Darblade, B., Héloir, M.-C., & Poinssot, B. (2018). The cell wall-derived xyloglucan is a new DAMP triggering plant immunity in *Vitis vinifera* and *Arabidopsis thaliana*. *Frontiers in Plant Science*, *9*. <https://doi.org/10.3389/fpls.2018.01725>
- Comellas, M. (2009). *Estudio de la interacción entre naranjo amargo y el virus de la tristeza de los cítricos*. Universitat Politècnica de València. PhD thesis. <https://doi.org/10.4995/Thesis/10251/7323>
- da Silva, M. C., Pinto, P. I. S., Guerra, R., Duarte, A., Power, D. M., & Marques, N. T. (2023). Gene transcripts responsive to drought stress identified in *Citrus macrophylla* bark tissue transcriptome have a modified response in plants infected by *Citrus tristeza virus*. *Scientia Horticulturae*, *307*, 111526. <https://doi.org/10.1016/j.scienta.2022.111526>
- Dalio, R. J. D., Magalhães, D. M., Rodrigues, C. M., Arena, G. D., Oliveira, T. S., Souza-Neto, R. R., Picchi, S. C., Martins, P. M. M., Santos, P. J. C., Maximo, H. J., Pacheco, I. S., De Souza, A. A., & Machado, M. A. (2017). PAMPs, PRRs, effectors and R-genes associated with citrus-pathogen interactions. *Annals of Botany*, *119*(5), 749–774. <https://doi.org/10.1093/aob/mcw238>
- Dawson, W., Garnsey, S., Tatineni, S., Folimonova, S., Harper, S., & Gowda, S. (2013). *Citrus tristeza virus*-host interactions. *Frontiers in Microbiology*, *4*, 88. <https://doi.org/10.3389/fmicb.2013.00088>
- Dawson, W. O., Bar-Joseph, M., Garnsey, S. M., & Moreno, P. (2015). *Citrus tristeza virus*: Making an ally from an enemy. *Annual Review of Phytopathology*, *53*, 137–155. <https://doi.org/10.1146/annurev-phyto-080614-120012>
- De Storme, N., & Geelen, D. (2014). Callose homeostasis at plasmodesmata: Molecular regulators and developmental relevance. *Frontiers in Plant Science*, *5*, 138. <https://doi.org/10.3389/fpls.2014.00138>
- Duarte, A., Fernandes, J., Bernardes, J., & Miguel, G. (2016). Citrus as a component of the mediterranean diet. *Journal of Spatial and Organizational Dynamics*, *IV*(4), 289–304.
- Folimonova, S. Y. (2020). *Citrus tristeza virus*: A large RNA virus with complex biology turned into a valuable tool for crop protection. *PLoS Pathogens*, *16*(4), e1008416. <https://doi.org/10.1371/journal.ppat.1008416>

- Folimonova, S. Y., Folimonov, A. S., Tatineni, S., & Dawson, W. O. (2008). *Citrus tristeza virus*: Survival at the edge of the movement continuum. *Journal of Virology*, 82(13), 6546–6556. <https://doi.org/10.1128/JVI.00515-08>
- Fry, S. C., Smith, R. C., Renwick, K. F., Martin, D. J., Hodge, S. K., & Matthews, K. J. (1992). Xyloglucan endotransglycosylase, a new wall-loosening enzyme activity from plants. *Biochemical Journal*, 282(Pt 3), 821–828. <https://doi.org/10.1042/bj2820821>
- Fu, S., Shao, J., Zhou, C., & Hartung, J. S. (2016). Transcriptome analysis of sweet orange trees infected with “*Candidatus Liberibacter asiaticus*” and two strains of *Citrus Tristeza Virus*. *BMC Genomics*, 17, 349. <https://doi.org/10.1186/s12864-016-2663-9>
- Fu, S., Shao, J., Zhou, C., & Hartung, J. S. (2017). Co-infection of sweet orange with severe and mild strains of *Citrus tristeza virus* is overwhelmingly dominated by the severe strain on both the transcriptional and biological levels. *Frontiers in Plant Science*. <https://doi.org/10.3389/fpls.2017.01419>
- Gómez-Muñoz, N., Velázquez, K., Vives, M. C., Ruiz-Ruiz, S., Pina, J. A., Flores, R., Moreno, P., & Guerri, J. (2017). The resistance of sour orange to *Citrus tristeza virus* is mediated by both the salicylic acid and RNA silencing defence pathways. *Molecular Plant Pathology*, 18(9), 1253–1266. <https://doi.org/10.1111/mpp.12488>
- Granato, L. M., Galdeano, D. M., D’Alessandre, N. D. R., Breton, M. C., & Machado, M. A. (2019). Callose synthase family genes plays an important role in the *Citrus* defense response to *Candidatus Liberibacter asiaticus*. *European Journal of Plant Pathology*, 155(1), 25–38. <https://doi.org/10.1007/s10658-019-01747-6>
- Harper, S. (2013). *Citrus tristeza virus*: evolution of complex and varied genotypic groups. *Frontiers in Microbiology*, 4. <https://doi.org/10.3389/fmicb.2013.00093>
- Hayashi, T., & Kaida, R. (2011). Functions of xyloglucan in plant cells. *Molecular Plant*, 4(1), 17–24. <https://doi.org/10.1093/mp/ssq063>
- Houston, K., Tucker, M. R., Chowdhury, J., Shirley, N., & Little, A. (2016). The plant cell wall: a complex and dynamic structure as revealed by the responses of genes under stress conditions. *Frontiers in Plant Science*, 7. <https://doi.org/10.3389/fpls.2016.00984>
- Iglesias, V. A., & Meins, F. J. (2000). Movement of plant viruses is delayed in a beta-1,3-glucanase-deficient mutant showing a reduced plasmodesmatal size exclusion limit and enhanced callose deposition. *The Plant Journal: For Cell and Molecular Biology*, 21(2), 157–166. <https://doi.org/10.1046/j.1365-313x.2000.00658.x>
- Karasev, A. V., Boyko, V. P., Gowda, S., Nikolaeva, O. V., Hilf, M. E., Koonin, E. V., Niblett, C. L., Cline, K., Gumpf, D. J., & Lee, R. F. (1995). Complete sequence of the *Citrus tristeza virus* RNA genome. *Virology*, 208(2), 511–520. <https://doi.org/10.1006/viro.1995.1182>
- Kaur, G. (2019). A review of XET enzymes, current applications and future trends. *International Journal of Latest Technology in Engineering, Management & Applied Science (IJLTEMAS)*, VIII(XI), 52–55.
- Kloth, K. J., & Kormelink, R. (2020). Defenses against virus and vector: a phloem-biological perspective on RTM- and SLII-mediated resistance to potyviruses and aphids. *Viruses*, 12(2). <https://doi.org/10.3390/v12020129>
- Korkmaz, S., Cevik, B., Onder, S., Koc, K., & Bozan, O. (2008). Detection of *Citrus tristeza virus* (CTV) from Satsuma Owari mandarins (*Citrus unshiu*) by direct tissue blot immunoassay (DTBIA), DAS-ELISA, and biological indexing. *New Zealand Journal of Crop and Horticultural Science*, 36(4), 239–246. <https://doi.org/10.1080/01140670809510240>
- Kozieł, E., Otulak-Kozieł, K., & Bujarski, J. J. (2021). Plant cell wall as a key player during resistant and susceptible plant-virus interactions. *Frontiers in Microbiology*, 12, 656809. <https://doi.org/10.3389/fmicb.2021.656809>
- Lee, J.-Y., & Lu, H. (2011). Plasmodesmata: The battleground against intruders. *Trends in Plant Science*, 16(4), 201–210. <https://doi.org/10.1016/j.tplants.2011.01.004>
- Li, W., Hartung, J. S., & Levy, L. (2006). Quantitative real-time PCR for detection and identification of *Candidatus Liberibacter* species associated with citrus huanglongbing. *Journal of Microbiological Methods*, 66(1), 104–115. <https://doi.org/10.1016/j.mimet.2005.10.018>
- Li, W., Zhao, Y., Liu, C., Yao, G., Wu, S., Hou, C., Zhang, M., & Wang, D. (2012). Callose deposition at plasmodesmata is a critical factor in restricting the cell-to-cell movement of *Soybean mosaic virus*. *Plant Cell Reports*, 31(5), 905–916. <https://doi.org/10.1007/s00299-011-1211-y>
- Liu, Y., Heying, E., & Tanumihardjo, S. A. (2012). History, global distribution, and nutritional importance of citrus fruits. *Comprehensive Reviews in Food Science and Food Safety*, 11(6), 530–545. <https://doi.org/10.1111/j.1541-4337.2012.00201.x>
- Madroñero, J., Rodrigues, S. P., Antunes, T. F. S., Abreu, P. M. V., Ventura, J. A., Fernandes, A. A. R., & Fernandes, P. M. B. (2018). Transcriptome analysis provides insights into the delayed sticky disease symptoms in *Carica papaya*. *Plant Cell Reports*, 37(7), 967–980. <https://doi.org/10.1007/s00299-018-2281-x>
- Marwal, A., & Gaur, R. K. (2020). Host plant strategies to combat against viruses effector proteins. *Current Genomics*, 21(6), 401–410. <https://doi.org/10.2174/1389202921999200712135131>
- Munir, N., Hameed, A. A., Haq, R., & Naz, S. (2019). Biochemical changes in cultivars of sweet oranges infected with *Citrus tristeza virus*. *Brazilian Journal of Biology*, 79(4), 742–748. <https://doi.org/10.1590/1519-6984.193791>
- Nedukha, O. M. (2015). Callose: Localization, functions, and synthesis in plant cells. *Cytology and Genetics*, 49(1), 49–57. <https://doi.org/10.3103/S0095452715010090>
- Otulak-Kozieł, K., Kozieł, E., & Lockhart, B. E. L. (2018). Plant cell wall dynamics in compatible and incompatible potato response to infection caused by *Potato Virus Y* (PVY<sup>NTN</sup>). *International Journal of Molecular Sciences*, 19(3). <https://doi.org/10.3390/ijms19030862>
- Pfaffl, M. W., Tichopad, A., Prgomet, C., & Neuvians, T. P. (2004). Determination of stable housekeeping genes, differentially regulated target genes and sample integrity: BestKeeper–Excel-based tool using pair-wise correlations. *Biotechnology Letters*, 26(6), 509–515. <https://doi.org/10.1023/b:bile.0000019559.84305.47>
- Piršelová, B., & Matušíková, I. (2013). Callose: the plant cell wall polysaccharide with multiple biological functions. *Acta Physiologiae Plantarum*, 35(3), 635–644. <https://doi.org/10.1007/s11738-012-1103-y>

- Ruiz-Ruiz, S., Moreno, P., Guerri, J., & Ambrós, S. (2007). A real-time RT-PCR assay for detection and absolute quantitation of *Citrus tristeza virus* in different plant tissues. *Journal of Virological Methods*, *145*(2), 96–105. <https://doi.org/10.1016/j.jviromet.2007.05.011>
- Sharples, S. C., Nguyen-Phan, T. C., & Fry, S. C. (2017). Xyloglucan endotransglucosylase/hydrolases (XTHs) are inactivated by binding to glass and cellulosic surfaces, and released in active form by a heat-stable polymer from cauliflower florets. *Journal of Plant Physiology*, *218*, 135–143. <https://doi.org/10.1016/j.jplph.2017.07.022>
- Shimizu, T., Satoh, K., Kikuchi, S., & Omura, T. (2007). The repression of cell wall- and plastid-related genes and the induction of defense-related genes in rice plants infected with *Rice dwarf virus*. *Molecular Plant-Microbe Interactions*, *20*, 247–254. <https://doi.org/10.1094/MPMI-20-3-0247>
- Tatineni, S., Robertson, C. J., Garnsey, S. M., & Dawson, W. O. (2011). A plant virus evolved by acquiring multiple nonconserved genes to extend its host range. *Proceedings of the National Academy of Sciences of the United States of America*, *108*(42), 17366–17371. <https://doi.org/10.1073/pnas.1113227108>
- Töller, A., Brownfield, L., Neu, C., Twell, D., & Schulze-Lefert, P. (2008). Dual function of *Arabidopsis* glucan synthase-like genes GSL8 and GSL10 in male gametophyte development and plant growth. *The Plant Journal: For Cell and Molecular Biology*, *54*(5), 911–923. <https://doi.org/10.1111/j.1365-313X.2008.03462.x>
- Vandesompele, D. P., Pattyn, F., Poppe, B., Van Roy, N., De Paep, A., & Speleman, F. (2002). Accurate normalization of real-time quantitative RT-PCR data by geometric averaging of multiple internal control genes. *Genome Biology*, *3*(7), 2279–2297. <https://doi.org/10.1186/gb-2002-3-7-research0034>
- Walker, G. P. (2022). Sieve element occlusion: Interactions with phloem sap-feeding insects. A review. *Journal of Plant Physiology*, *269*, 153582. <https://doi.org/10.1016/j.jplph.2021.153582>
- Wu, L., Han, Z., Wang, S., Wang, X., Sun, A., Zu, X., & Chen, Y. (2013). Comparative proteomic analysis of the plant-virus interaction in resistant and susceptible ecotypes of maize infected with *Sugarcane mosaic virus*. *Journal of Proteomics*, *89*, 124–140. <https://doi.org/10.1016/j.jprot.2013.06.005>
- Xie, B., Wang, X., Zhu, M., Zhang, Z., & Hong, Z. (2011). CalS7 encodes a callose synthase responsible for callose deposition in the phloem. *The Plant Journal*, *65*(1), 1–14. <https://doi.org/10.1111/j.1365-313X.2010.04399.x>
- Xie, F., Xiao, P., Chen, D., Xu, L., & Zhang, B. (2012). miR-DeepFinder: A miRNA analysis tool for deep sequencing of plant small RNAs. *Plant Molecular Biology*, *80*(1), 75–84. <https://doi.org/10.1007/s11103-012-9885-2>
- Yadav, R. K., & Chattopadhyay, D. (2014). Differential soybean gene expression during early phase of infection with *Mungbean yellow mosaic India virus*. *Molecular Biology Reports*, *41*(8), 5123–5134. <https://doi.org/10.1007/s11033-014-3378-0>
- Yang, Z. N., Mathews, D. M., Dodds, J. A., & Mirkov, T. E. (1999). Molecular characterization of an isolate of *Citrus tristeza virus* that causes severe symptoms in sweet orange. *Virus Genes*, *19*(2), 131–142. <https://doi.org/10.1023/a:1008127224147>
- Yang, C., Guo, R., Jie, F., Nettleton, D., Peng, J., Carr, T., Yeakley, J. M., Fan, J.-B., & Whitham, S. A. (2007). Spatial analysis of *Arabidopsis thaliana* gene expression in response to *Turnip mosaic virus* infection. *Molecular Plant-Microbe Interactions*, *20*(4), 358–370. <https://doi.org/10.1094/MPMI-20-4-0358>
- Zhang, J., Liu, N., Yan, A., Sun, T., Sun, X., Yao, G., Xiao, D., Li, W., Hou, C., Yang, C., & Wang, D. (2022). Callose deposited at soybean sieve element inhibits long-distance transport of *Soybean mosaic virus*. *AMB Express*, *12*(1), 66. <https://doi.org/10.1186/s13568-022-01402-0>
- Zheng, W., Ma, L., Zhao, J., Li, Z., Sun, F., & Lu, X. (2013). Comparative transcriptome analysis of two rice varieties in response to *Rice stripe virus* and small brown planthoppers during early interaction. *PLOS ONE*, *8*(12), e82126. <https://doi.org/10.1371/journal.pone.0082126>
- Zhou, Y., Liu, Y., Liu, K., Yang, F., & Zhou, C. (2017). Distribution and population structure of *Citrus tristeza virus* in *Poncirus trifoliata*. *Australasian Plant Pathology*, *46*(4), 351–355. <https://doi.org/10.1007/s13313-017-0498-8>

**Publisher's note** Springer Nature remains neutral with regard to jurisdictional claims in published maps and institutional affiliations.